On Using DNA-Trapping Electrophoresis To Increase the Resolution of DNA Sequencing Gels

Claude Desruisseaux,[†,‡] Gary W. Slater,[†] and Guy Drouin*[,‡]

Department of Physics and Department of Biology, University of Ottawa, Ottawa, Ontario K1N 6N5, Canada

Received April 15, 1998; Revised Manuscript Received July 21, 1998

ABSTRACT: It was previously shown that labeling one of the ends of single-stranded DNA molecules with streptavidin increases the interband separation of such DNA molecules when they are electrophoresed in denaturing polyacrylamide gels. This electrophoretic method was called DNA-trapping electrophoresis and seemed to be a promising method to increase the resolution of DNA sequencing ladders. Here, we show that this method requires inverted gel preruns to obtain optimal resolution, and we present a method to calculate the velocity of end-labeled DNA molecules in denaturing polyacrylamide gels. We use this method to elucidate the trapping mechanism and to characterize the electric field dependence of the critical size beyond which end-labeled DNA molecules are strongly trapped. Our results show that DNA-trapping electrophoresis cannot be used to increase the resolution of DNA sequencing ladders because, in the strong trapping regime, the bandwidths increase more than the gain in interband distances. On the other hand, it might be possible to use DNA-trapping electrophoresis to develop isoelectric focusing-like techniques using monotonic electric field gradients.

1. Introduction

DNA sequencing in polyacrylamide slab gels can typically resolve from 400 to 600 bases at single base resolution. This limit is due to the migration behavior of single-stranded DNA in polyacrylamide gels.[1,2] Optimized systems using long slab gels can resolve up to about 1000 bases.[3] However, reading accuracy decreases for molecular sizes larger than 600 bases and the thousand base limit is not always reachable.[4]

Because the current DNA sequencing technologies are widely regarded as one of the bottlenecks of the human genome project, new electrophoresis-based and other sequencing technologies have been suggested.[5−9] One such promising idea was suggested by Ulanovsky, Drouin, and Gilbert in a 1990 *Nature* paper.[10] These authors proposed to attach a large neutral label (such as the protein streptavidin, MW ≈ 52 000) to one end of the DNA molecules to be electrophoresed in a polyacrylamide gel. They noted that short streptavidin−DNA complexes (S-DNA) are only slightly retarded, while the velocity of S-DNA molecules larger than a certain critical size M^* (which depends on the applied electric field E) is dramatically reduced, thus increasing the mean interband spacing.[10] Although the proposed trapping electrophoresis (TE) process attracted a lot of attention in the DNA sequencing community, no new experimental results have appeared since. Theoretical studies have been published,[11−18] but no clear conclusions regarding the usefulness of TE have been reached. In this paper, we present the first in-depth study of TE and we establish its limitations for DNA separations. In particular, we show that TE's usefulness is severely restricted by current electrophoresis instruments.

* To whom correspondence should be addressed. Phone: (613) 562-5800 ext. 6052. Fax: (613) 562-5486. E-mail: guy@bio01.bio.uottawa.ca.

[†] Department of Physics.

[‡] Department of Biology.

2. Theory

Qualitatively, TE can be explained easily. We first note that when a S-DNA migrates in a random gel, its velocity is reduced due to the extra friction generated by the streptavidin label; in other words, a S-DNA molecule having M bases endures a frictional drag equivalent to $M + \alpha$ bases (α is evaluated below). In a gel, one has a wide range of pore sizes and structural defects. Under certain conditions (defined below), S-DNA molecules may stop migrating, at least temporarily, because they are trapped between gel fibers. Two trapping mechanisms have been proposed: (i) Ulanovsky[10] proposed the protein might get trapped in a fork-like protrusion of the gel (Figure 1A); we call this the "fork" trapping mechanism. (ii) The Slater−Drouin[13] and Viovy[16] groups, on the other hand, considered that trapping occurs when the flexible DNA chain enters a closed loop that is too narrow for the label (Figure 1B); we call this the "dead end" trapping mechanism. In either case, the S-DNA molecule clearly needs to move backward over a certain minimum distance L_0 in order to get out of the trap and resume migration in the field direction. Since the backward motion is due to Brownian motion, the detrapping time will increase (exponentially) with both the electric force (field intensity times charge of DNA) and the required distance L_0. Therefore, detrapping should be substantially easier for fork trapping (where L_0 is comparable to the mean pore size of the gel) than for dead end trapping (where L_0 is a function of the contour length of the DNA molecule). One of the goals of this article is to establish which trapping mode dominates the TE of S-DNA.

TE can be characterized by two time scales: the detrapping time τ_d and the time τ_0 it takes to get into a new trap. If V_0 is the velocity of the S-DNA complex between traps, its net velocity V in the presence of trapping is simply given by $V = V_0\tau_0/(\tau_0 + \tau_d)$. When $\tau_d \ll \tau_0$, trapping is ineffective and $V \approx V_0$: this defines

S0024-9297(98)00594-4 CCC: $15.00
Published on Web 09/03/1998

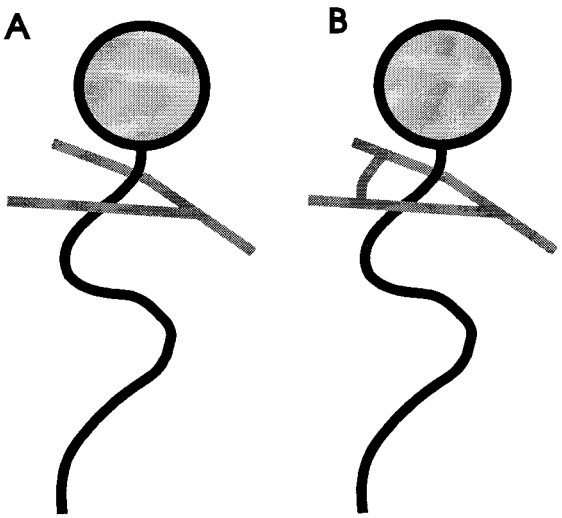

Figure 1. Schematic representation of the fork trapping mechanism proposed by Ulanovsky (A) and the dead end trapping mechanism proposed by the Slater−Drouin and Viovy (B) groups.

the weak trapping regime. When $\tau_d \gg \tau_0$, however, trapping dominates the dynamics and $V \approx V_0[\tau_0/\tau_d] \ll V_0$. The critical molecular size M^* that marks the transition from the weak to the strong trapping regime is thus the solution of the relation $\tau_0(M^*) = \tau_d(M^*)$. Another goal of this paper is to find the field dependence of the critical size M^*.

Slater and Villeneuve[11] used a modified version of the biased reptation model (BRM)[19−21] to carry out a computer simulation study of TE with dead end trapping. Their results showed a weak trapping regime where $V(M) \propto E/(M + \alpha)$, followed by a strong trapping regime for which $V(M) \propto \exp(-\beta M^3 E^2)$, where β is a constant. Therefore, this numerical model predicted that $M^* \sim E^{-2/3}$. We later developed an analytical model of TE[13] based on the BRM (again considering dead end trapping) to understand the behavior of both the net velocity V and the diffusion coefficient D. The problem could be described in terms of the dimensionless parameter $\Lambda = (2M/M_a)^{3/2}\epsilon$, where M_a is the amount of DNA contained in a mean gel pore of size a, and $\epsilon = M_a qEa/(2k_BT)$ is the scaled field intensity (here, k_B is the Boltzmann constant, T is the temperature, and q is the effective charge of one nucleotide). Note that $N = M/M_a$ thus defines the number of pores occupied by the DNA molecule. Trapping was predicted to be weak for $\Lambda < 1$ and strong for $\Lambda > 5$. This model also gave $M^* \sim E^{-2/3}$. The predicted velocity was consistent with the numerical results of Slater and Villeneuve,[11] while the model further predicted that D should increase exponentially with molecular size in the strong trapping regime (a very negative aspect of TE, of course). Using the same analytical approach, it is possible to show that fork trapping (where $L_0 \approx a$) would instead lead to $M^* \propto E^{-2}$. An intuitive explanation of the field dependence of M^* for both the fork and the dead end trapping modes is given in section 4.5, while a more complete derivation is included in Appendix A. Défontaines and Viovy[17] also developed an analytical reptation model of dead end TE where they allowed for the elongation of the reptation tube. They predicted numerous regimes for weak and strong tube elongation. In the limit of constant tube length (this approximation will be examined in the discussion), they also predicted that $M^* \sim E^{-2/3}$.

3. Materials and Methods

3.1. Polyacrylamide Gels. Eight percent polyacrylamide gels with a 19:1 acrylamide (BDH) to bisacrylamide (BDH) ratio were used. They contained 5 M urea (BDH), and a solution of 0.5 × TBE [44.5 mM Tris (BDH), 44.5 mM boric acid (BDH), 1 mM EDTA (BDH)] was used as the running buffer. The 0.1−0.4 mm thick gels were prepared on a Pharmacia-LKB Macrophor apparatus. Polymerization was initiated with the addition of 0.1% w/v ammonium persulfate (BDH) and 0.1% v/v TEMED (BDH), and the gels were left to polymerize at room temperature for at least 12 h.

3.2. DNA Samples. Radioactively labeled S-DNA 50 base pair ladders were prepared by mixing 1 μL of 50 base pair DNA ladder (1 μg/μL; Pharmacia), 3 μL of 5 × sequencing buffer (200 mM Tris−HCl, pH 7.5, 100 mM $MgCl_2$, 250 mM NaCl), 4.5 μL of biotin-14-dCTP (33 pmol/μL; Life Technologies), 3 μL of [α-^{32}P]TTP (3.3 μM; Amersham), 3 μL of distilled water, and 0.5 μL of Klenow (7.4 units/μL; Life Technologies), and this reaction was incubated for 15 min at room temperature. This reaction produced radioactive (α-^{32}P) double-stranded DNA fragments with a biotin molecule at both ends. We then added 5 μL of 0.5 M EDTA, 80 μL of TE (10 mM Tris, pH 8, 1 mM EDTA), and 1 μL of 0.1 mM streptavidin (diluted in TE; Boehringer Mannheim), and we incubated this reaction for 15 min at room temperature. This reaction allowed a streptavidin molecule to bind to each of the biotin molecules that were previously added at both ends of the DNA fragments. We finally added 100 μL of stop solution (95% formamide, 1% w/v xylene cyanol, 1% w/v bromophenol blue and 10 mM EDTA), and the samples were denatured at 65 °C for 5 min. This step led to the separation of the two DNA strands and therefore produced single-stranded DNA fragments having a streptavidin molecule at their 5′ end. Note that these denaturing conditions (incubation at 65 °C for 5 min in 50% v/v formamide) did not break the streptavidin−biotin bonds. These denatured samples were subsequently kept on ice until they were loaded on the gel. DNA sequencing reactions contained 1 pmol of M13mp18 single-stranded DNA, 2 pmol of a 5′-end biotinylated primer and were performed in a volume of 10 μL using T7 Sequencing Kits (Pharmacia). The reactions were stopped by adding 1 μL of 0.5 M EDTA, and 1 μL of 0.1 mM of streptavidin (diluted in TE; Boehringer Mannheim) was added. After a 15 min incubation period at room temperature, 12 μL of stop solution was added, and the samples were denatured as described above. The DNA fragments produced by these reactions were also radiolabeled (α-^{35}S) single-stranded DNA fragments having a streptavidin molecule at their 5′-end.

3.3. Electrophoresis Conditions. The running temperature (40 °C) was controlled through the thermostatic plate of the Pharmacia-LKB apparatus. Experiments with voltage ranging from 500 to 4000 V were performed on 18.5 cm long gels using a Fisher Biotech FB600 power supply. The gels were prerun at the selected field E (in V/cm) for at least 150/E hours (e.g., for 3 h at 50 V/cm) as we described previously.[22,23] Unless otherwise specified, the direction of the electric field during the prerun was opposite that of the electrophoresis. After that period of time, the electric current had fallen to about 40% of its initial value and remained constant during the whole electrophoresis (less than 2% variation). As discussed below, this procedure is necessary to obtain optimal results.

4. Results

4.1. Electric Field Gradients. The original report on TE,[10] as well as subsequent theoretical treatments,[11−14,17] clearly indicated that the gel electrophoretic mobility μ of large S-DNA molecules is strongly size- and field-dependent. The former is what makes TE an attractive method to improve separations; the latter, however, means that small field gradients along the direction of migration may have devastating effects. Unfortunately, it is known that the presence of urea can

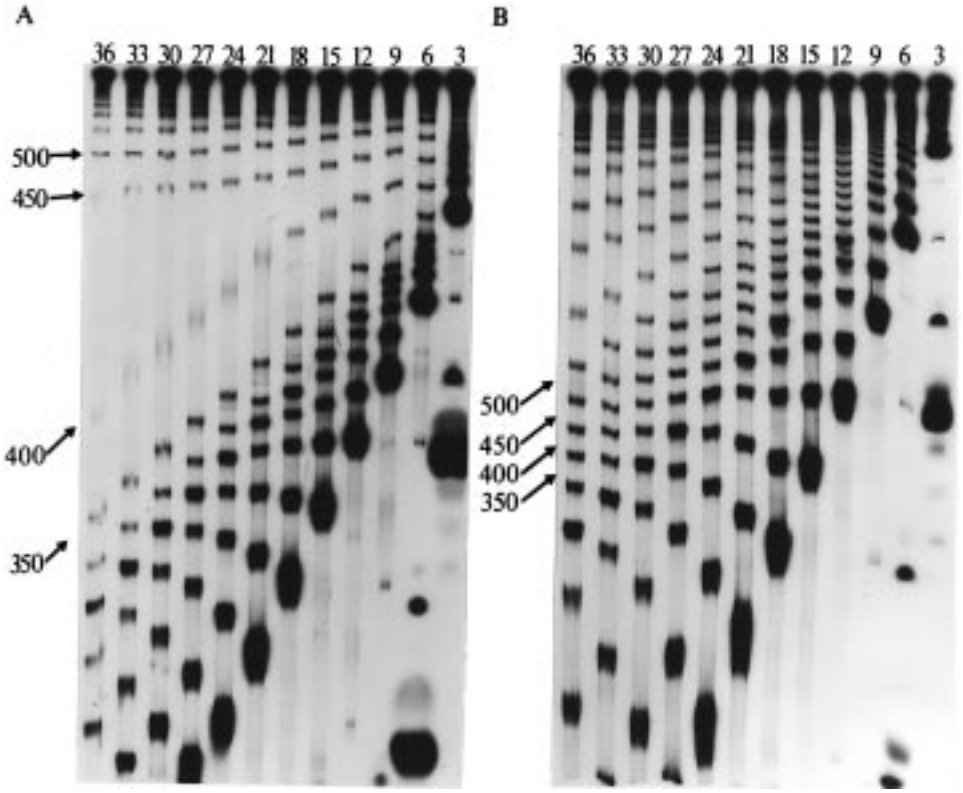

Figure 2. Autoradiogram of streptavidin−DNA molecules on gels subjected to a normal prerun (A) or an inverted prerun (B). Gels were run at 135 V/cm, and samples were loaded every 3 min.

lead to the formation of strong field gradients near the loading wells. This is due to the depletion of ions in this region of the gel.[22−24]

When the prerun is performed with the normal polarity (i.e., the polarity used for the separation), the field gradient forms over a period of a few hours and remains constant afterward. In a recent paper, we reported that the field actually reached about 200% of its mean value about 4−5 cm in front of the wells with the buffer used here.[24] It is obvious that if μ decreases exponentially with E in the strong trapping regime, most S-DNA molecules will accumulate where the local electric field E is maximum. We believe that the fact that the impact of the urea-generated field gradient was not considered explains why no further experimental article on TE were published after the original publication of Ulanovsky et al.[10]

After we recognized that the field gradients severely limited our empirical understanding of TE, we established an experimental method that would allow optimal results to be obtained. This method includes two main elements: (a) the prerun and (b) the loading procedure. We showed previously that a simple way to eliminate the gradient near the loading well is to prerun the gel with the opposite polarity until the current is stable.[22−24] The gradient then forms at the other end of the gel. Since it takes more than 2 h for the gradient to change position once the normal field polarity is applied (to carry out the separation), we have enough time to measure electrophoretic mobilities in spatially uniform electric fields. To obtain precise mobility values, we use the multiple loading method.[22−24] Briefly, we load identical samples in (≥3) adjacent wells every Δt minutes. We then measure the distance x_i migrated by a given molecular size for different migration times t_i. The slope of the resulting $x(t)$ vs t diagram gives the local velocity $V(x) = dx(t)/dt$, and indicates where the field is truly uniform. This procedure is absolutely required to obtain quantitative results for TE in denaturing polyacrylamide gels.

4.2. Normal vs Inverted Preruns. Figure 2A shows the autoradiogram for a 50 base S-DNA ladder electrophoresed in a 8% polyacrylamide, 5 M urea, 0.5×TBE gel when a normal prerun (field direction is the same during the prerun and the experiment) of 2 h was performed at 135 V/cm prior to the experiment. Since consecutive loadings were made every $\Delta t = 3$ min, the gel picture itself is a $x(t)$ vs t diagram. The velocities of the $M < 400$ base fragments are clearly higher at the beginning of the gel but reach a constant value about 5 cm beyond the loading wells (at the top of the picture). The behavior of the 400 base fragment is most interesting: its velocity is constant during the first 2 cm (first 6 min), then decreases for the next 2 cm (next 6 min), and finally increases again until it reaches a constant value in the middle of the gel. Note also that the width of this band increases very quickly in the region where the field is decreasing (from 18 to 21 min). We call this behavior band anti-focusing. It is worth noting that the width of the band does not increase as quickly when the band is in the region where the field is constant (beyond 21 min). Larger molecules ($M \geq 500$ bases) migrate until they reach the point where the local field intensity is high enough that they get completely trapped. Interestingly, the width of the 500 base fragment band decreases (it focuses) although the electric field increases in the region where it gets trapped. These results make it clear that unless one controls the field gradients, TE cannot be properly characterized, let alone exploited.

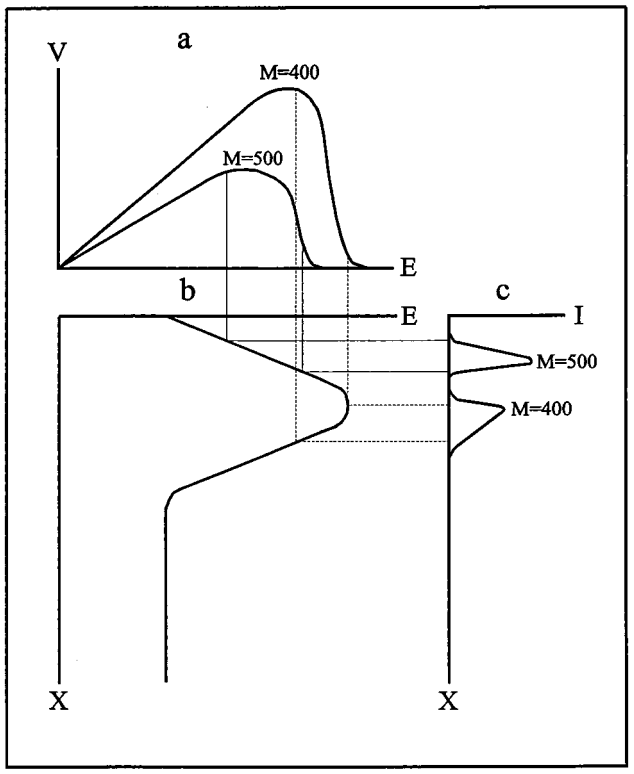

Figure 3. Schematic representation of (a) the velocity V vs the electric field (for fragments of 400 and 500 bases), (b) the electric field E vs position x, and (c) the density of molecules I vs position x.

Figure 2B shows the same experiment with an inverted prerun. The situation is much simpler. For instance, the velocity of all fragments is essentially uniform throughout the gel. This allows us to observe a remarkable increase in interband spacing in the 400−800 base range. Inverted preruns generate very small positive field gradients over a few centimeters near the loading wells and these field gradients will only affect extremely large fragments that will get trapped in this region.

Figure 3 shows a schematic representation of the complex situation observed when a normal prerun is used. Figure 3a provides a velocity V vs electric field E diagram for two different S-DNA sizes (400 and 500 bases). The local value $E(x)$ of the electric field intensity[24] along the direction of migration (x) is given in Figure 3b. Finally, Figure 3c presents the density of S-DNA fragments vs position x (i.e., the band shape). The plots share common axes with one another and thus provide a complete picture of the process.

We first note (Figure 3a) that the velocity increases linearly with E up to a certain critical value $E^*(M)$, beyond which it quickly decreases. Note that E^* is inversely proportional to M (see section 2). Figure 3b indicates that for a normal prerun, the local field reaches a maximum a few centimeters ahead of the loading wells and then converges toward a lower constant value in the middle of the gel. Figure 3c is essentially a convolution of Figure 3a,b for a case where the 400 base band (500 base band) is in the region where the electric field is decreasing (increasing). The field intensity is seen to be stronger at the tail of the 400 base band, while the field is weaker at the front of this band. Figure 3a then tells us that for the 400 base band $V_{front} > V_{tail}$, which means that the bandwidth will increase very quickly because of the local antifocusing field conditions. The situation is quite different for the 500 base band, which is located in the region where the field is increasing. We are now in the situation where $V_{front} < V_{tail}$, and the field gradient leads to band focusing (narrowing). Moreover, the diagram makes it clear that it is impossible for a 500 base fragment to cross the region of the electric field gradient because the field exceeds the critical value $E^*(M = 500)$ at one point. The latter acts like a fixed point. Finally, we note that both the focusing and the antifocusing bands must be asymmetric.

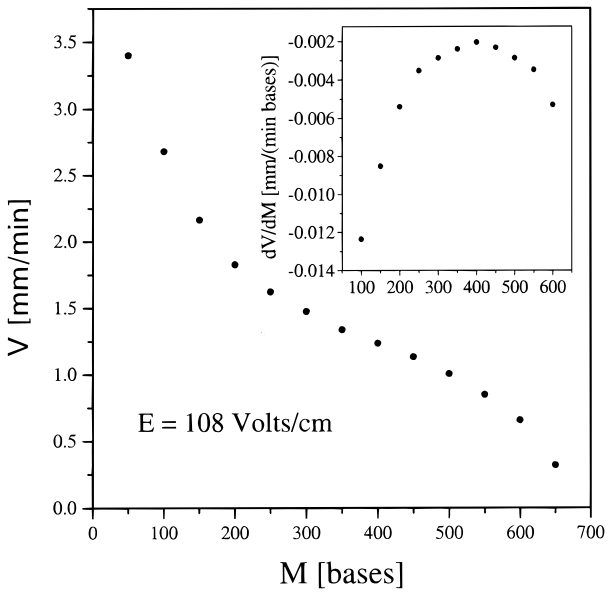

Figure 4. Velocity V vs molecular size M for an electric field $E = 108$ V/cm. Inset: dV/dM vs M.

In practice, the normal prerun is to be avoided because the bands either never get passed the field gradient (e.g., our $M \geq 500$ base band) or become extremely wide (e.g., our 400 base band). These results do not allow us to draw quantitative conclusions about TE and certainly do not give any useful separation. This is why inverted preruns are necessary for TE in denaturing polyacrylamide gels.

4.3. Determination of *M.** Using inverted preruns and multiple loadings, as described above, we can find the critical size M^* for a given applied field E. Figure 4 shows a plot of the velocity $V(M)$ vs M for a field of $E = 108$ V/cm. Instead of seeing the usual plateau for large DNA sizes,[1,2] we observe an inflection point for $M \approx 400$ bases, followed by a rapid decrease. The velocity is negligible for $M > 700$ bases. We define M^* as the value of the molecular size at the inflection point, a simple and practical choice. Therefore, M^* is found by locating the maximum on a dV/dM vs M plot (inset of Figure 4). Looking at Figure 2B, we see indeed that the bands get closer and closer as the molecular size increases below $M = 400$. Starting at $M = M^* = 400$, however, the interband spacing starts increasing for a while because of the effect of steric trapping. Finally, note that we see bands up to the loading wells, something that we do not see with normal DNA electrophoresis.

4.4. Weak vs Strong Trapping. Figure 5 shows a log−log plot of the electrophoretic mobility $\mu = V/E$ vs the applied field E for DNA molecular sizes ranging from 50 (top curve) to 700 bases (bottom curve). The

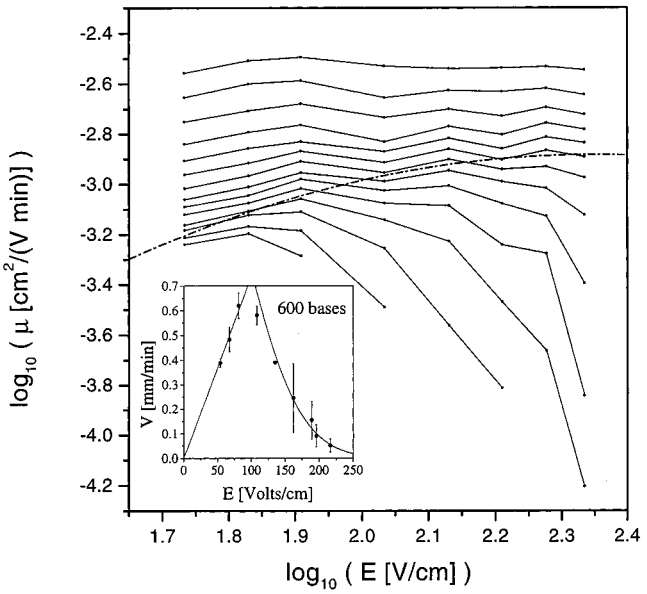

Figure 5. log−log plot of the mobility μ vs field intensity E (for molecules ranging from 50 (top) to 700 bases (bottom). The inset shows the velocity V vs E for a 600 base molecule. The dashed line delimits the weak (above) and the strong (below) trapping regimes.

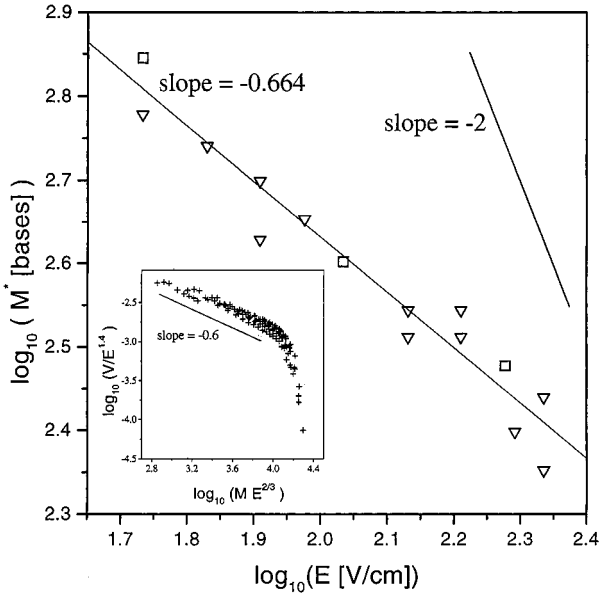

Figure 6. log−log plot of the critical molecular size M^* vs the field intensity E. Square points represent two identical results. The inset shows a log−log of $V/E^{1.4}$ vs $ME^{2/3}$, where the velocity V is expressed in mm/min and the electric field E is in V/cm.

mobility is approximately constant (hence $V \propto E$) for $M \leq 300$ bases, indicating that these molecules remain in the weak trapping regime for these fields. The $M > 350$ base molecules exhibit both the weak and the strong trapping regime. Indeed, their mobilities are observed to be constant up to a certain critical electric field and to decrease beyond this value. The broken curve shows the separation between the weak and strong trapping regimes as given by the $M^*(E)$ values found using the method described in section 4.3. As an example, the inset of Figure 5 shows a plot of the velocity V vs the electric field E for a 600 base fragment. The velocity increases linearly with E for $E < 100$ V/cm; the slope of the straight line fit then gives the trapping-free mobility $\mu = 7.39 \times 10^{-4}$ cm^2/(V min). However, the velocity of the 600 base fragment then decreases very quickly for $E > 100$ V/cm. The tail of the V vs E graph was fitted to the function exp(−constant $\times E^2$), the analytical form predicted by our dead end trapping model[13] and previous computer simulations.[11] The resulting fit is reasonable, but the error bars are so large that equally good agreement can be obtained using many other functions.

4.5. Critical Size M^* vs the Electric Field E. Figure 6 shows a log−log plot of the critical size M^* vs the applied electric field E. The straight line fit has slope of −0.664, fully consistent with the relation $M^* \propto E^{-2/3}$ that we predicted for the dead end trapping model shown in Figure 1b. Despite the scatter of the points, our results clearly rule out fork trapping,[10] which predicts a slope of −2.

The fact that $M^* \propto E^{-2}$ for fork trapping and $M^* \propto E^{-2/3}$ for dead end trapping can be understood using simple scaling arguments. For any trapping system, the time τ_d to get out of a trap is a function of W/k_BT, where W is the work necessary to get out of the trap, k_B is the Boltzman constant, and T is the temperature. This can be written as $\tau_d = \tau^{(0)} f(W/k_BT)$, where $f(W/k_BT \ll 1) \cong 1$ (weak trapping regime). The structure of the function $f(W/k_BT)$ in the limit where $W/k_BT \gg 1$ (strong trapping) is given by $\ln[f(W/k_BT \gg 1)] \propto W/k_BT$ (the Kramer approximation).[16−18] Therefore, $W/k_BT \cong 1$ defines the critical value for the transition between weak and strong trapping. For both trapping mechanisms, the force holding the molecule in the trap is $F \propto Eh_x$, where E is the electric field and h_x is the end-to-end distance of the DNA molecules in the direction parallel to the field.[11−23] Since the DNA molecules retain their random-walk conformations (i.e., $h_x \propto M^{1/2}$) in such experiments, we obtain $W/k_BT \propto EM^{1/2}L_0$, where L_0 is the distance over which the molecule must move (backward) to get out of the trap. For fork trapping, L_0 does not depend on the molecular size and we have $W/k_BT \propto EM^{1/2}$, giving $M^* \propto E^{-2}$. On the other hand, for dead end trapping, the molecule needs to move completely out of the trap, i.e., $L_0 \propto M$, and we obtain $W/k_BT \propto EM^{3/2}$ and $M^* \propto E^{-2/3}$.

4.6. A Universal Curve. The inset of Figure 6 shows a log−log plot of $V/E^{1.4}$ vs $ME^{2/3}$ for all the data that we have obtained (i.e., for all values of E and M used in our study). A satisfactory universal curve is obtained. The −0.6 slope observed for small values of $ME^{2/3}$ corresponds to the trapping-free regime where $V \propto E$. The abrupt decrease found for $ME^{2/3} \gtrsim 10^{4.1}$ corresponds to the strong trapping regime and indicates that $M^*E^{2/3} \approx 10^{4.1}$ or $M^* \approx 10^{4.1}E^{-2/3}$, which is consistent with the dead end trapping mechanism.

5. Discussion

Unfortunately, the fact that the mobility of S-DNA molecules is strongly field-dependent implies that even small field inhomogeneities can lead to detrimental antifocusing effects. Since large field gradients do form naturally in the presence of urea,[24] TE cannot be used with normal preruns for DNA sequencing. This is one of the important results of this article, and likely explains why new TE experimental results have not been published since the original publication of Ulanovsky et al.[10] Here, we have demonstrated that inverted preruns are necessary to obtain optimal TE separations, and their use has allowed us to carry out the first systematic experimental study of TE. Our results agree nicely with the predicted scaling law M^*

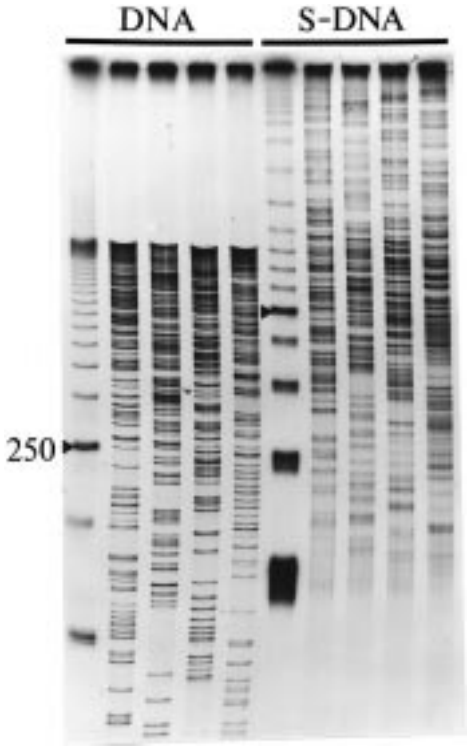

Figure 7. Autoradiogram of 50 base ladders and sequencing reaction (T, C, G, and A) for DNA and S-DNA. The gel was run at 135 V/cm for 30 min. The two arrows mark the position of the $M = 250$ base DNA and S-DNA molecules.

$\sim E^{-2/3}$, and we found that all our TE data could be represented by a universal curve (inset of Figure 6).

Our experimental setup did not allow us to measure reliable diffusion coefficients, a necessary ingredient to calculate the resolution. Therefore, to determine whether the resolution of DNA sequencing ladders could be improved using TE, we electrophoresed DNA and S-DNA sequencing reactions and 50-base ladders on a polyacrylamide gel with an inverted prerun (Figure 7). For unmodified DNA, the interband spacing decreases, but the bands are narrower for large molecular size DNAs. Moreover, there are no DNA bands in the first 5−6 cm of gel because the $M > 1000$ base fragments comigrate at that position. For the streptavidin−DNA (S-DNA) molecules, the interband spacing decreases for $M < 400$ bases and then increases for a while before it decreases again. As a result, the 400−650 base range is much better separated for S-DNA, and we find S-DNA bands over the whole gel (this is therefore a better use of the gel). However, the bandwidths, which decrease for S-DNAs smaller than 400 bases, increase for larger molecules, in qualitative agreement with the predictions of our model.[13] This increased diffusion is due to the trapping mechanism and it greatly reduces the benefits of the increased interband spacing. In other words, the gain in interband separation is not enough to increase the overall resolution compared to unmodified DNA because the bands are broader.

On the other hand, the remarkable increase in interband spacing could possibly be used for specific applications, such as testing for point mutations or for accurate sizing. Another way to exploit TE would be to use monotonic field gradients where the electric field is increasing with the position throughout the gel. This could be achieved using gels where the gel thickness decreases from the loading end of the gel to the bottom of the gel. In such a gel, a S-DNA molecule of size M would migrate up to its own focusing point, i.e., where the local critical molecular size $M^*(E(x)) = M$. This behavior was observed on Figure 2A for the $M = 500$ base fragment. This modified TE process would be analogous to protein isoelectric focusing.

From our results, we can also estimate a few microscopic parameters related to TE. The persistence length of single-stranded DNA is $p \approx 1.9$ nm in 0.5×TBE.[25] Using this value and the results of Rousseau et al.,[26] we estimate that the mean pore size of our 8% polyacrylamide gels is about $a = 6.2$ nm. The size and shape of streptavidin were studied by Hendrickson et al.[27] who report that streptavidin is effectively a sphere of radius $r_s \approx 2.5$ nm. It is possible to obtain a rough estimate of the fraction f_s of pores of size $x < r_s$ by using Lumpkin et al.[21] distribution of pore sizes $g(x)\,dx = 2\pi\lambda x \exp(-\pi\lambda x^2)\,dx$, where $\lambda = 1/(4a^2)$. The calculation gives

$$f_s = \int_0^{r_s} g(x)\,dx \approx \frac{1}{8.3}$$

This indicates that there is a fair amount of small pores. The fact that $p \cong a/3$ suggests that DNA is fairly stiff inside a pore; this may explain why our results agree with a theory that assumes that DNA is inextensible in its tube.

We know that for DNA molecules, the velocity scales such as $V_{DNA}(M) = C/M$ while for a S-DNA molecule $V_{S-DNA}(M) = C/(M + \alpha)$ (where C is a constant) so that $V_{DNA}(M)/V_{S-DNA}(M) = 1 + \alpha/M$. We have estimated α by plotting $V_{DNA}(M)/V_{S-DNA}(M)$ vs $1/M$ for molecules in the reptation/weak trapping regime to obtain $\alpha = 125 \pm 25$ (not shown). This can also be estimated from Figure 7 where we see that the 50 base S-DNA molecule comigrates with the ≈175 base DNA molecule. This is in contrast with the value $\alpha \approx 23$ reported for free-flow electrophoresis of S-DNA.[5] Clearly, the presence of the gel greatly increases the friction generated by the uncharged label, possibly due to collisions and hydrodynamic (confinement) effects.

In conclusion, TE of S-DNA is characterized by a strongly field- and size-dependent electrophoretic mobility. While the latter makes it a promising method to increase separation, the former makes it extremely sensitive to field inhomogeneities. The presence of urea-related field gradients explains why it has been so difficult until now to reach definite conclusions about the usefulness and mechanisms of TE. Our study shows that the reptation model provides a satisfactory description of TE. Unfortunately, the latter predicted that increased band broadening would not make TE a good technique to improve the resolution of DNA sequencing ladders, a prediction that we have verified. Therefore, TE's usefulness would be limited to specific applications. We have suggested that with monotonic field gradients, TE could be transformed into an interesting isoelectric focusing-like technique. Alternatively, pulsed fields could be used to modulate the effect of the steric trapping.[10,14,18] However, it is extremely important to note that unless the field is uniform in space, pulsed fields are not likely to be of any use. Recently, Griess and Serwer[29] have demonstrated that ZIFE pulses[28] can be used to separate DNA and labeled DNA molecules because of a clever ratchet dynamical effect.[30] The latter, unfortunately, cannot be exploited for DNA sequencing purposes.

Acknowledgment. The authors would like to thank Hongji Ren, Grant Nixon, Tarso B. L. Kist, Shehre-Banoo Malik, and two anonymous reviewers for constructive comments on this paper. This work was supported by Research Grants of the National Science and Engineering Research Council of Canada to G.D. and G.W.S.

Appendix A

Here, we follow the biased reptation model of Slater et al.[13] The detrapping problem is similar to the diffusion of a particle starting on a reflecting wall at $s = 0$ (the trap) and trying to reach an absorbing wall at $s = -L_0$ while having a velocity $(\partial s/\partial t) = \epsilon h_x/\tau_B > 0$, where h_x is the end-to-end distance of S-DNA in the field direction, $\tau_B = a^2/2D_s$ is the Brownian time, $D_s = k_BT/[\xi(N + \alpha)]$ is the curvilinear diffusion coefficient, and N is the number of gel pores occupied by the S-DNA. The particle must move backward (i.e., against the electric forces) over a distance L_0 in order to leave the steric trap. The general solution of eq 9 of Slater et al.[13] for the mean detrapping time τ_d is

$$\frac{\tau_d}{\tau_B} = \frac{{L_0}^2}{a^2}\left[\frac{2}{3}\sqrt{\frac{\Omega}{\pi}}H(\Omega) + \frac{1}{\Omega}(1 - e^{\Omega}) - \sqrt{\frac{\pi}{-\Omega}}\,\mathrm{erf}(\sqrt{-\Omega})\right] \quad \text{(A1)}$$

Here, the functions $\mathrm{erf}(\Omega)$ and $H(\Omega)$ are defined by

$$\mathrm{erf}(\Omega) = \frac{2}{\sqrt{\pi}}\int_0^{\Omega} e^{-y^2}\,dy \quad \text{(A2)}$$

$$H(\Omega) = \sum_{k=0}^{\infty}\frac{\Omega^k\Gamma(5/2)}{(k+1)\Gamma(k+5/2)} \quad \text{(A3)}$$

where $\Gamma(x)$ is the gamma function and $\Omega \equiv 2N\epsilon^2{L_0}^2/3a^2$. For small Ω's, we have

$$\frac{\tau_d}{\tau_B} \approx \frac{{L_0}^2}{a^2}\left[1 + \frac{2}{3\sqrt{\pi}}\sqrt{\Omega} + \frac{\Omega}{6} + ...\right] \quad \text{(A4)}$$

Ω is thus the gauge that tells us if we are in the weak ($\Omega < 1$) or strong ($\Omega > 1$) trapping regimes. Dead end trapping implies that $L_0 = Na$ (detrapping requires moving backward over the entire tube length) so that $\Omega = 2N^3\epsilon^2/3$. For fork trapping,[10] we have $L_0 \approx a$; i.e., detrapping requires moving backward over the distance of the order of a single pore and does not depend on the molecular size of the S-DNA fragments. In this case, $\Omega = 2N\epsilon^2/3$. Therefore, strong trapping will occur for molecules larger than $N^* = 3/(2\epsilon^2) \sim 1/\epsilon^2$ (or $M^* \sim 1/E^2$) for fork trapping or for molecules larger than $N^* = (3/(2\epsilon^2))^{1/3} \sim 1/\epsilon^{2/3}$ (or $M^* \sim 1/E^{2/3}$) for dead end trapping.

References and Notes

(1) Slater, G. W.; Drouin, G. *Electrophoresis* **1992**, *13*, 574−582.
(2) Grossman, P. D.; Menchen, S.; Hershey D. *GATA* **1992**, *9* (1), 9−16.
(3) Zimmermann, J.; Wiemann, S.; Voss, H.; Schwager, C.; Ansorge W. *BioTechniques* **1994**, *17*, 302−307.
(4) McDonald, L. A.; Kelley, J. M.; Brandon, R. C.; Adams, M. D. *BioTechniques* **1995**, *19*, 464−471.
(5) Heller, C.; Slater, G. W.; Mayer, P.; Dovichi, N.; Pinto, D.; Viovy, J.-L.; Drouin, G. *J. Chromatogr. A* **1998**, *806*, 113−121.
(6) Mayer, P.; Slater, G. W.; Drouin G. *Anal. Chem.* **1994**, *66*, 1777−1780.
(7) Davis, L. M.; Fairfield, F. R.; Harger, C. A.; Jett, J. H.; Keller, R. A.; Hahn, J. H.; Krakowski, L. A.; Marrone, B. L.; Martin, J. C.; Nutter, H. L.; Ratliff, R. L.; Shera, E. B.; Simpson, D. J.; Soper, S. A. *GATA* **1991**, *8* (1), 1−7.
(8) Lindsay, S. M.; Philipp, M. *GATA* **1991**, *8* (1), 8−13.
(9) Chee, M.; Yang, R.; Hubbel, E.; Berno, A.; Huang, X. C.; Stern, D.; Winkler, J.; Lockhart, D. J.; Morris, M. S.; Fodor, S. P. A. *Science* **1996**, *274*, 610−614.
(10) Ulanovsky, L.; Drouin G.; Gilbert, W. *Nature* **1990**, *343*, 190−192.
(11) Slater, G. W.; Villeneuve, C. *J. Polym. Sci. B: Polym. Phys.* **1992**, *30*, 1451−1457.
(12) Desruisseaux, C.; Slater, G. W. *Phys. Rev. E* **1994**, *49*, 5885−5888.
(13) Slater, G. W.; Desruisseaux, C.; Villeneuve, C.; Guo, H. L.; Drouin G. *Electrophoresis* **1995**, *16*, 704−712.
(14) Desruisseaux, C.; Slater, G. W. *Electrophoresis* **1996**, *17*, 623−632.
(15) Ulanovsky, L. *Methods Enzymol.* **1992**, *216*, 54−68.
(16) Défontaines, A.-D.; Viovy, J.-L. In *Proceedings of the First International Conference on Electrophoresis, Supercomputing and the Human Genome*; Cantor, C. R., Lim, H. A., Eds.; World Scientific: Singapore, 1991; pp 286−312.
(17) Défontaines, A.-D.; Viovy, J.-L. *Electrophoresis* **1993**, *14*, 8−17.
(18) Défontaines, A.-D.; Viovy, J.-L. *Electrophoresis* **1994**, *15*, 111−119.
(19) Slater, G. W.; Noolandi, J. *Biopolymers* **1986**, *25*, 431−454.
(20) Slater, G. W. *Electrophoresis* **1993**, *14*, 1−7.
(21) Lumpkin, O. J.; Déjardin, P.; Zimm, B. H. *Biopolymers* **1985**, *24*, 1573−1593.
(22) Mayer, P.; Slater, G. W.; Drouin G. *Appl. Theor. Electrophoresis* **1993**, *3*, 147−155.
(23) Slater, G. W.; Mayer, P.; Drouin G. *Methods Enzymol.* **1993**, *270*, 272−295.
(24) Desruisseaux, C.; Slater, G. W.; Drouin G. *Electrophoresis* **1998**, *19*, 627−634.
(25) Tinland, B.; Pluen, A.; Sturm, J.; Weill G. *Macromolecules* **1997**, *30*, 5763−5765.
(26) Rousseau, J.; Drouin, G.; Slater, G. W. *Phys. Rev. Lett.* **1997**, *79*, 1945−1948.
(27) Hendrickson, W. A.; Pähler, A.; Smith, J. L.; Satow, Y.; Merritt, E. A.; Phizackerley R. P. *Proc. Natl. Acad. Sci. U.S.A.* **1989**, *86*, 2190−2194.
(28) Turmel, C.; Brassard, E.; Forsyth, R.; Hood, K.; Slater, G. W.; Noolandi, J. In *Electrophoresis of Large DNA Molecules, Theory and Applications*; Lai, E., Birren, B. W., Eds.; Cold Spring Harbor Laboratory Press: New York, 1990; pp 101−131.
(29) Griess, G. A.; Serwer, P. *Biophys. J.* **1998**, *74* (2), A71.
(30) Desruisseaux, C.; Slater, G. W.; Kist, T. B. L. Submitted to *Biophys. J.*

MA980594E